



Published in final edited form as:

J Vasc Surg. 2017 September ; 66(3): 891–901. doi:10.1016/j.jvs.2016.07.127.

AN ENDOVASCULAR MODEL OF ISCHEMIC MYOPATHY FROM PERIPHERAL ARTERY DISEASE

Chandler A. Long, MD, PhD^{#1}, Lucas H. Timmins, PhD^{#2}, Panagiotis Koutakis, PhD³, Traci T. Goodchild, PhD⁴, David J. Lefer, PhD⁴, Iraklis I. Pipinos, MD³, George P. Casale, PhD³, and Luke P. Brewster, MD, PhD^{1,5}

¹Emory University School of Medicine, Department of Surgery; Atlanta GA

²Emory University School of Medicine, Department of Radiology and Imaging Sciences; Atlanta GA

³ University of Nebraska Medical Center; Omaha NE

⁴ Cardiovascular Center of Excellence, Louisiana State University School of Medicine, New Orleans, LA

⁵ Atlanta VA Medical Center, Surgical and Research Services

These authors contributed equally to this work.

Abstract

Objective—Peripheral arterial disease (PAD) is a significant age-related medical condition with limited pharmacologic options. Severe PAD, termed critical limb ischemia (CLI), can lead to amputation. Skeletal muscle is the end organ most affected by PAD leading to ischemic myopathy and patient debility. Currently, there are not any therapeutics to treat ischemic myopathy, and proposed biologic agents have not been optimized due to a lack of pre-clinical models of PAD. Since a large animal model of ischemic myopathy may be useful in defining the optimal dosing and delivery regimens, the objective was to create and characterize a swine model of ischemic myopathy that mimics patients with severe PAD.

Methods—Yorkshire swine (N = 8) underwent acute right hindlimb ischemia via endovascular occlusion of the external iliac artery. The effect of ischemia on limb function, perfusion, and the degree of ischemic myopathy was quantified by weekly gait analysis, arteriography, hindlimb blood pressures, femoral artery duplex ultrasounds, and histologic examination. Animals were terminated at 5 (N = 5) and 6 (N = 3) weeks post-operatively. Ossabaw swine (N = 8) fed a high fat diet were utilized as a model of metabolic syndrome for comparison of arteriogenic recovery and validation of ischemic myopathy.

Corresponding Author: Luke P. Brewster, MD, PhD, Division of Vascular Surgery, Woodruff Memorial Building, 101 Woodruff Circle, Suite 5105, Atlanta, GA 30322, lbrewst@emory.edu, Telephone: 404.727.8329, Fax: 404.712.5826.

Publisher's Disclaimer: This is a PDF file of an unedited manuscript that has been accepted for publication. As a service to our customers we are providing this early version of the manuscript. The manuscript will undergo copyediting, typesetting, and review of the resulting proof before it is published in its final citable form. Please note that during the production process errors may be discovered which could affect the content, and all legal disclaimers that apply to the journal pertain.

This paper was presented at the 2016 Southern Association for Vascular Surgery, Cancun, Mexico, January 13 – 16, 2016.

Results—There was persistent ischemia in the right hindlimb and occlusion pressures were significantly depressed compared to the untreated left hindlimb out to 6 weeks (SBP 31 ± 21 versus 83 ± 15 , respectively; $P=0.0007$). The blood pressure reduction resulted in a significant increase of ischemic myopathy in the gastrocnemius muscle in the treated limb. Gait analysis revealed a functional deficit of the right hindlimb immediately post-occlusion that improved rapidly over the first 2 weeks. Peak systolic velocity values in the right common femoral artery were severely diminished throughout the entire study ($P<0.001$), and the hemodynamic environment post-occlusion was characterized by low and oscillatory wall shear stress. Finally, the internal iliac artery on the side of the ischemic limb underwent significant arteriogenic remodeling (1.8x baseline) in the Yorkshire, but not the Ossabaw swine model.

Conclusions—This model utilizes endovascular technology to produce the first durable large animal model of ischemic myopathy. Acutely (first 2 weeks) this model is associated with impaired gait but no tissue loss. Chronically (2-6 weeks), this model delivers persistent ischemia resulting in ischemic myopathy similar to that seen in PAD patients. This model may be of use for testing novel therapeutics including biologic therapies for promoting neovascularization and arteriogenesis.

INTRODUCTION

Peripheral arterial disease (PAD) is an age-related disease affecting 12 – 14% of the population¹ that significantly increases cardiovascular morbidity and mortality². With increasing ischemia, PAD patients have increasing ischemic myopathy, gait disturbance, rest pain, and/or tissue loss, resulting in increased risk for major amputation^{3,4}. Patients with PAD have abnormal skeletal muscle morphology from persistent ischemia and this leads to limb dysfunction⁵. In more severe manifestations, PAD can progress to critical limb ischemia (CLI); here there is inadequate perfusion to meet resting tissue demands. CLI is a devastating disease affecting an estimated 500,000 to 1 million patients annually, and up to 10% of PAD patients over 50 years of age will develop CLI within 5 years of diagnosis⁶.

There are limited therapeutic options for PAD patients beyond those prescribed for cardiovascular disease⁷ and none target ischemic myopathy directly⁸. Further while surgical revascularization restores perfusion and can be life and limb saving⁹, it is typically reserved for patients who fail medical therapy or who have progressed to CLI. In these patients, surgical revascularization may not always be enough to prevent amputation¹⁰, and the amputation rate can still approach 30% at one year¹¹. Since 33 – 50% of CLI patients do not have suitable anatomy or available conduit for revascularization¹², major amputation remains the only treatment option for many patients¹³. Given the increased incidence and prevalence of PAD/CLI worldwide, this disease is likely to impose an even greater burden on patient health in the years to come^{14,15}. Thus, there is a critical need to develop novel therapies to limit ischemic myopathy and promote limb salvage.

Biologic therapies are a promising approach for PAD patients. Here cells, genes, or angiogens could improve wound healing, restore perfusion to ischemic tissue, and/or improve ischemic myopathy and function. However the optimal delivery methods and dosing strategies are not known and cannot be tested in these trials¹⁶. Thus the lack of

translational model for new pharmaceutical and biologic agents may play a role in the failure of some clinical trials^{17, 18}. A large animal model of ischemic myopathy from PAD may be useful in preclinical testing of these promising therapeutics. The choice of a large animal for this study is in accord with the FDA guidance for investigators regarding the development of cellular therapies for cardiovascular disease. Here the FDA accepts the limitations of small animal models and states that, “large animal models should provide information on the safety and activity of cellular products and delivery systems, leading to the selection of a potentially safe starting dose for a Phase 1 clinical trials”¹⁹.

To date, published large animal models of PAD have been limited by rapid collateralization which is not seen in PAD patients clinically and diminishes the timeframe of ischemia to less relevant durations. In addition many models contaminate the tissue with iatrogenic local tissue injury²⁰. Obviously the prevention of rapid collateralization will provide for a more durable ischemic state, and a sustained plateau period of limb ischemia is desirable for testing new agents. Importantly, the degree of ischemia must not be disabling or accompanied by severe morbidity so that test therapeutic agents can be adequately tested. Endovascular techniques can also limit local tissue trauma. Thus, the objective of this study was to develop a large animal model of ischemic myopathy from PAD for use in testing novel therapeutics. This model utilizes endovascular occlusion of the external iliac artery in two breeds of swine (one with and one without metabolic syndrome), and this work describes the return of ambulatory function and quantifies arterial perfusion and ischemic myopathy over 5-6 weeks post induction of hindlimb ischemia.

METHODS

Animals and animal care

Sexually mature female Yorkshire swine (N = 8), 6 – 8 months of age [average weight 52.9 Kg (\pm 3.2Kg)], were obtained from a local vendor. Similarly aged Ossabaw swine (N = 8) were obtained from Indiana University. The Ossabaw swine were fed a high fat diet, which leads to a metabolic syndrome phenotype^{21, 22}. All animals were handled in compliance with the “Guide for the Care and Use of Laboratory Animals,” published by the National Institute of Health and according to the guidelines of the Emory University Institutional Animal Care and Use Committee.

Swine Diet and Feeding—Yorkshire Swine were acclimated for one week prior to experimentation and fed standard chow diet. For 6 months prior to experimentation, Ossabaw swine were fed 1 kg/day atherogenic obese diet (KT324, Test Diet) comprised of 2% cholesterol, 17% coconut oil, 2.5% corn oil, and 0.7% sodium cholate for 6 months as published^{21, 22}.

Peri-operative care—Pre-operative analgesic buprenorphine (0.15mg for each pig) was given along with peri-operative antibiotics cefazolin (1000 mg). Peri-operative heparin was given to keep activated clotting time >300 seconds during the procedure. Post-operatively, buprenorphine (0.15 – 0.3 mg) was given immediately after the procedure and intermittently at the discretion of the veterinary team as warranted for animal discomfort.

In vivo model of CLI in Yorkshire swine

Swine were anesthetized and intubated under standard conditions, and then maintained on isoflurane gas and ventilator through the entirety of each operation²⁰. Pre-operative hindlimb blood pressure indices (HLI) and duplex ultrasound (US) of the common femoral arteries were recorded on both hindlimbs.

Arterial access—The first two Yorkshire pigs underwent percutaneous access to the ipsilateral right common femoral artery, but we converted to an open carotid artery exposure to avoid manipulation of tissue in the access limb of the remaining animals.

Induction of Hindlimb ischemia—The right common carotid artery was accessed over a starter wire with a 9 French (9F) sheath, and the sheath was secured to the carotid artery with 2-0 silk suture ligatures. A 6F vertebral catheter was then advanced over a .035" Bentson wire into the descending aorta with the use of fluoroscopy to navigate the aortic arch. The catheter was advanced over a wire to the site of the aortic trifurcation. Approximately 6mL of 50% strength Iovue contrast was used for each arteriogram, totaling 10 arteriograms for the initial procedure. We first imaged the aortic trifurcation (Figure 1). Bilateral external iliac arteries (EIA) and the common iliac artery were identified. The left EIA was then selected for imaging the common femoral/superficial femoral artery in two planes, and then the below knee runoff separately. The right side was treated in the same manner, but the right EIA was then re-imaged to demonstrate its ostia, the lateral circumflex branch, and the medial profunda branch for proper placement of the stent (Figure 1). The Bentson wire was advanced into the superficial femoral artery, and the catheter was removed. A GORE® Viabahn® covered stent (7 or 8mm × 10 cm; W.L. Gore & Associates, Inc., Flagstaff, AZ) was then placed in the right EIA/common femoral artery, functionally excluding the orifices of the circumflex iliac and profunda artery. Proper placement and exclusion of the lateral circumflex and profunda arteries was subsequently confirmed by selective arteriogram. The vertebral catheter was then re-introduced to the EIA over the wire to position it midway into the stent. A 10 mm Amplatzer™ vascular plug (St. Jude Medical, St. Paul, MN) was then delivered through the vertebral catheter and deployed in its “double bubble” configuration in the proximal stent. Completion aortograms were then performed two minutes after deployment to confirm occlusion and capture outflow bilaterally. At the conclusion of the procedure, the right common carotid artery was ligated with 2-0 silk sutures, and the wound closed in 2 layers. Finally, completion HLI and ultrasound measurements were performed as above. The animal was then awakened and recovered by our veterinarian team prior to departure to its cage. The left hind limb’s arterial supply was not manipulated and served as the control limb for comparison.

In vivo CLI model in Ossabaw swine—Obese female swine (N = 8) were treated similarly, but the EIA was stented with a 6mm × 10 cm Viabahn stent, due to the smaller size of the arteries, and an 8mm Amplatzer plug was used. Of note, these animals were used as placebo control animals from a recent publication²¹. These animals were used to demonstrate how our model can be used in swine with features more representative of clinical diseases relevant to PAD (here metabolic syndrome). Unpublished data (ischemic myopathy and arteriogenesis) from the above study is included in this study as comparison

with Yorkshire animals to demonstrate the reliability of this model in two distinct strains of swine.

Hindlimb index (HLI) measurement and calculation—HLI were measured using a continuous wave Doppler of the tarsal arteries and a pediatric blood pressure cuff at the ankle joint. After successful identification of the arterial signal, the cuff pressure was then rapidly increased ~30mmHg above occlusion of the signal. The cuff was then slowly released until the return of the arterial signal was identified. The ischemic limb (right) occlusion pressure was then compared to the normal limb (left) as the HLI. Animals were anesthetized for immediate post procedure and terminal measurements; they were sedated for the interim measurements.

Duplex ultrasound of common femoral and superficial femoral arteries—Duplex US (Vivid *i*, i12L-RS Probe, GE Healthcare) was performed and recorded for each artery. Short and long axis views of the SFA on both legs were acquired with multiple doppler planes looking for flow distal to the implant site. Pulse wave doppler was acquired in both short and long axis to quantify the peak systolic and end diastolic velocity of blood flow. Animals were anesthetized for immediate post procedure and terminal measurements; they were sedated for the interim measurements.

Serial examinations of animals after induction of hindlimb ischemia—All Yorkshire swine underwent weekly duplex ultrasound measurements of the common femoral and superficial femoral arteries, and HLI. Videos of the gait of the Yorkshire swine were captured weekly in the animal vivarium to capture gait abnormalities using a Canon EOS Rebel T3 camera.

Terminal arteriogram—At 5 weeks post-occlusion, all swine underwent left common carotid artery access and repeat arteriograms as described above. The common femoral arteries were imaged at 0 and 30 degrees. This allows for reconstruction of the vessel and quantification of wall shear stress (WSS) values.

Euthanasia and tissue collection—After completion of all the studies the Yorkshire swine were euthanized under deep anesthesia with a lethal dose of potassium chloride. The animals were then brought to the necroscopy room for tissue collection.

Manual and Automatic Quantification of Ischemic Myopathy

Gastrocnemius muscle samples were collected from the animals during necroscopy. Sections from the gastrocnemius of the swine were obtained and stained with Hematoxylin-Eosin. Manual slide review was performed on the Ossabaw swine gastrocnemius and plantaris muscles in a blinded fashion as published.^{5, 23} Automated quantification of Yorkshire swine was developed using a custom Matlab (Mathworks, Natick, MA) subroutine to quantify muscle morphologic features. Micrographs were acquired on a standard inverted microscope (IX51 inverted microscope, Olympus America, Inc., Melville, NY) using a phase-contrast objective (X10 UPLFLN series, numerical aperture: 0.3, Olympus America, Inc.). Image processing techniques (e.g., filtering, size exclusion, edge detection) were applied to each

image to extract myofiber tissue and quantify myofiber areas. An image of a standard stage micrometer (0.01 mm markings) was acquired with identical imaging equipment and settings to accurately determine image resolution.

Arteriogram image analysis

Time-of-flight and wall shear stress (WSS) analyses—Arterial flow was measured directly from the initiation of contrast bolus in the distal aorta until time of contrast entering the common femoral artery. Measurements compared right (occluded EIA) to left (normal EIA) at completion arteriogram. WSS values were calculated pre-CLI and at 35 days post-CLI from the acquired imaging and hemodynamic data. Common femoral artery diameters were extracted from the angiographic data at peak systole. Pulsatile doppler derived velocity values were digitized from the recorded data. Under the assumptions for Poiseuille flow, which results in a reduced form of the Navier-Stokes equations that govern fluid dynamics, WSS values were calculated.

Arteriogenesis in the internal iliac artery—The porcine anatomy is favorable to this model as the ipsilateral internal iliac artery is derived from the common iliac artery. Internal iliac artery (IIA) diameters were measured pre-occlusion and at 5 weeks post-occlusion in the Yorkshire and Ossabaw swine. Diameters were analyzed by multiple diameter measurements. Comparisons were made between pre/post diameters between the right (ipsilateral) and left (contralateral) IIA.

Statistical Analysis

All data in this study are expressed as the mean \pm SD. Differences in data between the groups were compared using Prism 4 (GraphPad Software) with Student's unpaired, two-tailed t-test when only two groups were compared. A P-value < 0.05 was considered statistically significant. Other statistical analyses are noted specifically in the appropriate results section.

RESULTS

Peri-operative events

One Yorkshire pig died during the initial arteriogram procedure. In that instance, the procedure was aborted prior to deployment of stent and the animal killed because of persistent bradycardia and hypotension. Necropsy revealed a restrictive pericarditis as the cause of death. This animal was replaced with a subsequent animal for a total of 8 Yorkshire pigs that completed the study.

Hindlimb index (HLI) and gait disturbance

The ischemic hindlimb occlusion pressure was significantly depressed in the right versus left leg out to 6 weeks (SBP 31 ± 21 versus 83 ± 15 , respectively; $P = 0.0007$). Here the HLI was depressed throughout the time course of this study allowing at least a 28-day therapeutic testing window (Figure 2A, B). Qualitatively, all animals had grossly normal gait after 2 weeks of ischemia, but a subtle gait disturbance persisted at weeks 4-5 post hind limb

ischemia. Here animals had 6.6 (± 3.5) abnormal steps out of 21 (± 2) steps during a 10 meter walk video.

US velocity of common femoral artery

The peak systolic velocity of the common femoral artery was severely depressed throughout the time course of this study ($P < 0.001$ at all time points). The greatest increase in velocity occurred between 1 and 2 weeks post occlusion. Velocities in the right hindlimb disappeared and slowly recovered over 5 weeks to 38% of their baseline values. These velocities directly correlated to the gain in HLI values over time. Interestingly, the end diastolic velocity (EDV) was not significantly different between groups (Figure 2C, D).

Ischemic myopathy

For Yorkshire swine, the muscle myofiber area was decreased in the ischemic compared to non-treated limbs ($P < 0.05$). Representative images of the range in severity of ischemic myopathy is demonstrated in Yorkshire swine as compared to human patients in Figure 3. Importantly the myofiber area was significantly decreased in the ischemic compared to normal limb (Figure 4). Similar results were obtained in the fat fed Ossabaw group with good correlation between manual and Matlab-generated quantification of ischemic myopathy (Figure 5).

Time of flight flow and wall shear stress analyses

At time of acute occlusion, there was no flow identified in the right common femoral and superficial femoral arteries. At terminal arteriogram (5 weeks post-ischemia), there was reconstitution of flow to these arteries by branches of the profunda to geniculate arteries (Supplemental Videos 1 and 2). Here there was significant delay in filling of the femoral arteries on the right compared to left side (2.8 seconds versus 0.3 seconds, respectively; $P = 0.003$). In addition, the reversal of flow with retrograde filling of these arteries from the geniculate arteries signifies oscillatory WSS in this artery. Interestingly, at 35-days post ischemia, the left leg (control) continues to demonstrate normal WSS values, but the right (ischemic) limb exhibits very low WSS values (Figure 6).

Arteriogenesis

There was robust arteriogenesis of the ipsilateral Yorkshire IIA. There was more than a 50% increase in the diameter of the IIA in the post-intervention angiograms compared to the pre-intervention images. Interestingly, this was not present in the fat-fed Ossabaw swine (Figure 7).

DISCUSSION

The need to develop animal models of PAD/CLI that reflect the human condition has been recognized for many years. These models could be used to answer questions about whether autologous or allogeneic cells are optimal for certain regenerative therapies^{18, 24}, the type of cells used²⁵⁻²⁷, optimal dosing strategies and delivery methods²⁸, and the benefits/limitations of cellular expansion versus immediate delivery of cellular therapies²⁹.

In this study, we introduced and characterized a novel porcine model of ischemic myopathy that has sustained severe ischemia using endovascular occlusion of the EIA and exclusion of its collateral vessels by means of a covered stent graft and vascular plug. This model improves upon existing animal models²⁰ with regard to the degree and duration of ischemia, and it obviates the tissue damage associated with open arterial ligation³⁰⁻³². Additionally, modular ischemia (supra or infra-inguinal) can be added to this model and induced downstream as described in the literature^{33, 34}. Arterial occlusions in the supra- and infra-inguinal region behave differently, and endovascular therapies in animal models have not been well examined. The only existing studies in the literature were an acute study that looked at distal arterial embolization³⁵ and a laser-occlusion of the iliac artery. The latter had substantial perioperative mortalities and the report focused on the arterial injury, not the impact of distal ischemia³⁶. In contrast the model described here shares many similarities to the ischemic myopathy seen in PAD patients^{5, 37, 38}. Still there are existing animal models of ischemic myopathy that are already established^{33, 39}, and the strengths and limitations of current models have been recently reviewed^{20, 40}. These models have been particularly effective for the study of collateral production, but they do not produce the degree or duration of ischemia (mostly recovered within 2 weeks post-ischemia) required for testing novel pharmacologic or regenerative therapies^{30-33, 41}. Thus the useful features of this model for PAD translational research are: 1) endovascular delivery of ischemia to avoid local tissue injury, 2) sustained limb ischemia with skeletal myopathy in calf muscles that can be quantified using semi-automated methodology, 3) altered WSS that may be useful in understanding how fluid mechanics inform arterial remodeling in large animals, and 4) demonstration of both robust arteriogenic remodeling in the ipsilateral internal iliac artery of Yorkshire swine and diminished response in the fat-fed Ossabaw swine that mimic metabolic syndrome. This difference in arteriogenic potential between the Yorkshire and Ossabaw is very similar to that identified clinically in patients with metabolic syndrome⁴². Thus, this model can be tuned to animals like the fat-fed Ossabaw swine to add features like metabolic syndrome, which may impact the specifics of dosing strategies, choice of pharmaceuticals tested, and/or the delivery strategy and choice of cells for regenerative therapies.

PAD patients have significant ischemic myopathy^{5, 37} and this model demonstrates ischemic changes similar to that seen in patients⁴³. Thus this model is well equipped to test agents designed to improve muscle perfusion and function. Also the WSS values are similar to that seen in patients on the unaffected (left) side and low WSS values that are consistent with significant arterial pathology in the common femoral artery on the affected (right) side. Therefore pathologic arterial remodeling that occurs in areas of low and oscillatory WSS can be tested in these arteries.

This model does have some specific limitations. First, the onset of ischemia is not the typical progressive atherosclerotic occlusion of PAD. The initial ischemic injury is acute with hallmarks of acute limb ischemia. However after two weeks these animals have recovered the ability to ambulate, the systolic blood pressure ratios are consistent with those seen clinically in PAD, and the ischemic injury to the muscle at termination are very consistent to those seen in PAD patients. Still it is unclear how much the HLI will recover over time. It is possible that animals will behave similar to patients with inflow disease and plateau at a resting ABI of ~0.8. Regardless it remains to be seen how long significant ischemia persists

in our model, and it may be desirable to have a prolonged ischemic period for testing some therapeutic agents. Obviously exercising these animals may bring on a precipitous drop in these ABI measurements. Further given the modular nature of endovascular approaches, a longer therapeutic window could be built into this model by delayed occlusion of the ipsilateral internal iliac artery. This would mandate the right limb was perfused by cross pelvic collateralization. Also testing of this model was restricted to female swine. PAD is a significant medical condition for women^{44, 45}, and the female sex is frequently understudied in the translational testing of therapeutics. This model may also have utility in therapeutic testing of pharmaceuticals that are not involved in regenerative medicine. Here, this model has been tested in fat-fed Ossabaw to test nitrite delivery on angiogenesis and coronary vasoreactivity in these animals^{21, 22}. Finally the quantification of gait disturbance in this model was under-developed and can be better analyzed with existing technology⁴⁶.

CONCLUSION

This large animal translational model of ischemic myopathy may be useful to the testing of regenerative therapy. This model can be applied across different types of swine, which can be chosen according to the clinical condition investigators are interested in translating. Future work in applying this model to the testing of novel therapeutics may be useful in identifying the optimal dosages and delivery of these agents.

Supplementary Material

Refer to Web version on PubMed Central for supplementary material.

ACKNOWLEDGEMENTS

Funding: Emory/Georgia Institute of Technology Regenerative Engineering and Medicine (LB), which is supported in part by PHS Grant UL1TR000454 from the Clinical and Translational Science Award Program, National Institutes of Health, National Center for Advancing Translational Sciences. NHLBI KO8HL119592 & Society for Vascular Surgery/American College of Surgeons Scientific Development Grant (LB), American Heart Award Innovative Research Grant IRG14740001 (LB), Emory Department of Surgery Startup Funds (LB).

We would like to acknowledge the generous donation of product from the W.L. Gore Inc. We would also like to acknowledge the contributions of Dr. Tatiana Chadid Santamaria for her assistance in the procedures and collection of tissues, and Dr. Haiyan Li, Mr. Faizan Boghani and Ms. Katie Kuo for their assistance with the gait analysis and collection of tissues. Finally, we acknowledge the technical assistance of Michael Sweet and the team at T3 laboratories for their organization and assistance with the completion of these experiments.

REFERENCES

1. Shamma NW. Epidemiology, classification, and modifiable risk factors of peripheral arterial disease. *Vasc Health Risk Manag.* 2007; 3:229–234. [PubMed: 17580733]
2. Golomb BA, Dang TT, Criqui MH. Peripheral arterial disease: Morbidity and mortality implications. *Circulation.* 2006; 114:688–699. [PubMed: 16908785]
3. Fowkes FG, Housley E, Cawood EH, Macintyre CC, Ruckley CV, Prescott RJ. Edinburgh artery study: Prevalence of asymptomatic and symptomatic peripheral arterial disease in the general population. *Int J Epidemiol.* 1991; 20:384–392. [PubMed: 1917239]
4. Da Silva A, Widmer LK, Ziegler HW, Nissen C, Schweizer W. The basle longitudinal study: Report on the relation of initial glucose level to baseline ecg abnormalities, peripheral artery disease, and subsequent mortality. *J Chronic Dis.* 1979; 32:797–803. [PubMed: 511968]

5. Koutakis P, Myers SA, Cluff K, Ha DM, Haynatzki G, McComb RD, et al. Abnormal myofiber morphology and limb dysfunction in claudication. *J Surg Res.* 2015; 196:172–179. [PubMed: 25791828]
6. Norgren L, Hiatt WR, Dormandy JA, Nehler MR, Harris KA, Fowkes FG, Group TIW. Inter-society consensus for the management of peripheral arterial disease (tasc ii). *J Vasc Surg.* 2007; 45(Suppl S):S5–67. [PubMed: 17223489]
7. Chung J, Timaran DA, Modrall JG, Ahn C, Timaran CH, Kirkwood ML, et al. Optimal medical therapy predicts amputation-free survival in chronic critical limb ischemia. *J Vasc Surg.* 2013; 58:972–980. [PubMed: 23993439]
8. Abu Dabrh AM, Steffen MW, Asi N, Undavalli C, Wang Z, Elamin MB, et al. Nonrevascularization-based treatments in patients with severe or critical limb ischemia. *J Vasc Surg.* 2015; 62:1330–1339. e1313. [PubMed: 26409842]
9. Barshes NR, Menard MT, Nguyen LL, Bafford R, Ozaki CK, Belkin M. Infrainguinal bypass is associated with lower perioperative mortality than major amputation in high-risk surgical candidates. *J Vasc Surg.* 2011; 53:1251–1259. e1251. [PubMed: 21292432]
10. Goodney PP, Likosky DS, Cronenwett JL. Predicting ambulation status one year after lower extremity bypass. *J Vasc Surg.* 2009; 49:1431–1439. e1431. [PubMed: 19497502]
11. Hirsch AT, Haskal ZJ, Hertzner NR, Bakal CW, Creager MA, Halperin JL, et al. Acc/aha 2005 practice guidelines for the management of patients with peripheral arterial disease (lower extremity, renal, mesenteric, and abdominal aortic): A collaborative report from the american association for vascular surgery/society for vascular surgery, society for cardiovascular angiography and interventions, society for vascular medicine and biology, society of interventional radiology, and the acc/aha task force on practice guidelines (writing committee to develop guidelines for the management of patients with peripheral arterial disease): Endorsed by the american association of cardiovascular and pulmonary rehabilitation; national heart, lung, and blood institute; society for vascular nursing; transatlantic inter-society consensus; and vascular disease foundation. *Circulation.* 2006; 113:e463–654. [PubMed: 16549646]
12. Powell RJ, Simons M, Mendelsohn FO, Daniel G, Henry TD, Koga M, et al. Results of a double-blind, placebo-controlled study to assess the safety of intramuscular injection of hepatocyte growth factor plasmid to improve limb perfusion in patients with critical limb ischemia. *Circulation.* 2008; 118:58–65. [PubMed: 18559703]
13. Abu Dabrh AM, Steffen MW, Undavalli C, Asi N, Wang Z, Elamin MB, et al. The natural history of untreated severe or critical limb ischemia. *J Vasc Surg.* 2015; 62:1642–1651. e1643. [PubMed: 26391460]
14. Sampson UK, Norman PE, Fowkes FG, Aboyans V, Yanna S, Harrell FE Jr. et al. Global and regional burden of aortic dissection and aneurysms: Mortality trends in 21 world regions, 1990 to 2010. *Global heart.* 2014; 9:171–180. e110. [PubMed: 25432126]
15. Barshes NR, Belkin M, Collaborators MS. A framework for the evaluation of "value" and cost-effectiveness in the management of critical limb ischemia. *J Am Coll Surg.* 2011; 213:552–566. e555. [PubMed: 21943802]
16. Powell RJ. Update on clinical trials evaluating the effect of biologic therapy in patients with critical limb ischemia. *J Vasc Surg.* 2012
17. Teraa M, Conte MS, Moll FL, Verhaar MC. Critical limb ischemia: Current trends and future directions. *Journal of the American Heart Association.* 2016:5.
18. Teraa M, Sprengers RW, Schutgens RE, Slaper-Cortenbach IC, van der Graaf Y, Algra A, et al. Effect of repetitive intra-arterial infusion of bone marrow mononuclear cells in patients with no-option limb ischemia: The randomized, double-blind, placebo-controlled rejuvenating endothelial progenitor cells via transcutaneous intra-arterial supplementation (juventas) trial. *Circulation.* 2015; 131:851–860. [PubMed: 25567765]
19. FDA. Guidance for industry: Cellular therapies for cardiovascular disease. 2010
20. Ziegler MA, Distasi MR, Bills RG, Miller SJ, Alloosh M, Murphy MP, et al. Marvels, mysteries, and misconceptions of vascular compensation to peripheral artery occlusion. *Microcirculation.* 2010; 17:3–20. [PubMed: 20141596]

21. Polhemus DJ, Bradley JM, Islam KN, Brewster LP, Calvert JW, Tao YX, et al. Therapeutic potential of sustained-release sodium nitrite for critical limb ischemia in the setting of metabolic syndrome. *Am J Physiol Heart Circ Physiol.* 2015; 309:H82–92. [PubMed: 25910804]
22. Bradley JM, Islam KN, Polhemus DJ, Donnarumma E, Brewster LP, Tao YX, et al. Sustained release nitrite therapy results in myocardial protection in a porcine model of metabolic syndrome with peripheral vascular disease. *Am J Physiol Heart Circ Physiol.* 2015; 309:H305–317. [PubMed: 25957218]
23. Thompson JR, Swanson SA, Haynatzki G, Koutakis P, Johanning JM, Reppert PR, et al. Protein concentration and mitochondrial content in the gastrocnemius predicts mortality rates in patients with peripheral arterial disease. *Ann Surg.* 2015; 261:605–610. [PubMed: 24670845]
24. Powell RJ, Marston WA, Berceci SA, Guzman R, Henry TD, Longcore AT, et al. Cellular therapy with ixmyelocel-t to treat critical limb ischemia: The randomized, double-blind, placebo-controlled restore-cli trial. *Mol Ther.* 2012; 20:1280–1286. [PubMed: 22453769]
25. Teraa M, Sprengers RW, van der Graaf Y, Peters CE, Moll FL, Verhaar MC. Autologous bone marrow-derived cell therapy in patients with critical limb ischemia: A meta-analysis of randomized controlled clinical trials. *Ann Surg.* 2013; 258:922–929. [PubMed: 23426345]
26. Smadja DM, d'Audigier C, Guerin CL, Mauge L, Dizier B, Silvestre JS, et al. Angiogenic potential of bm mscs derived from patients with critical leg ischemia. *Bone Marrow Transplant.* 2012; 47:997–1000. [PubMed: 21986637]
27. Gremmels H, Teraa M, Quax PH, den Ouden K, Fledderus JO, Verhaar MC. Neovascularization capacity of mesenchymal stromal cells from critical limb ischemia patients is equivalent to healthy controls. *Mol Ther.* 2014; 22:1960–1970. [PubMed: 25174586]
28. Landazuri N, Levit RD, Joseph G, Ortega-Legaspi JM, Flores CA, Weiss D, et al. Alginate microencapsulation of human mesenchymal stem cells as a strategy to enhance paracrine-mediated vascular recovery after hindlimb ischaemia. *J Tissue Eng Regen Med.* 2012
29. Bourin P, Bunnell BA, Casteilla L, Dominici M, Katz AJ, March KL, et al. Stromal cells from the adipose tissue-derived stromal vascular fraction and culture expanded adipose tissue-derived stromal/stem cells: A joint statement of the international federation for adipose therapeutics and science (ifats) and the international society for cellular therapy (isct). *Cytherapy.* 2013; 15:641–648. [PubMed: 23570660]
30. Voskuil M, van Royen N, Hoefler IE, Seidler R, Guth BD, Bode C, et al. Modulation of collateral artery growth in a porcine hindlimb ligation model using mcp-1. *Am J Physiol Heart Circ Physiol.* 2003; 284:H1422–1428. [PubMed: 12505873]
31. Buschmann IR, Voskuil M, van Royen N, Hoefler IE, Scheffler K, Grundmann S, et al. Invasive and non-invasive evaluation of spontaneous arteriogenesis in a novel porcine model for peripheral arterial obstructive disease. *Atherosclerosis.* 2003; 167:33–43. [PubMed: 12618266]
32. Grundmann S, Hoefler I, Ulusans S, Bode C, Oesterle S, Tijssen JG, et al. Granulocyte-macrophage colony-stimulating factor stimulates arteriogenesis in a pig model of peripheral artery disease using clinically applicable infusion pumps. *J Vasc Surg.* 2006; 43:1263–1269. [PubMed: 16765251]
33. Tang GL, Chang DS, Sarkar R, Wang R, Messina LM. The effect of gradual or acute arterial occlusion on skeletal muscle blood flow, arteriogenesis, and inflammation in rat hindlimb ischemia. *J Vasc Surg.* 2005; 41:312–320. [PubMed: 15768015]
34. Brown MD, Kelsall CJ, Milkiewicz M, Anderson S, Hudlicka O. A new model of peripheral arterial disease: Sustained impairment of nutritive microcirculation and its recovery by chronic electrical stimulation. *Microcirculation.* 2005; 12:373–381. [PubMed: 16020083]
35. Margovsky A, Bobryshev YV, Chambers AJ, Iliopoulos J, Lord RS. Small vessel ischaemia induced by microbead embolization in the sheep hind limb. *The Australian and New Zealand journal of surgery.* 1998; 68:592–598. [PubMed: 9715138]
36. White CJ, Ramee SR, Card HG, Abrahams LA, Svinarich JT, Wade CE, et al. Laser angioplasty: An atherosclerotic swine model. *Lasers Surg Med.* 1988; 8:318–321. [PubMed: 2969072]
37. Weiss DJ, Casale GP, Koutakis P, Nella AA, Swanson SA, Zhu Z, et al. Oxidative damage and myofiber degeneration in the gastrocnemius of patients with peripheral arterial disease. *Journal of translational medicine.* 2013; 11:230. [PubMed: 24067235]

38. Koutakis P, Weiss DJ, Miserlis D, Shostrom VK, Papoutsis E, Ha DM, et al. Oxidative damage in the gastrocnemius of patients with peripheral artery disease is myofiber type selective. *Redox biology*. 2014; 2:921–928. [PubMed: 25180168]
39. Naehle CP, Steinberg VA, Schild H, Mommertz G. Assessment of peripheral skeletal muscle microperfusion in a porcine model of peripheral arterial stenosis by steady-state contrast-enhanced ultrasound and doppler flow measurement. *J Vasc Surg*. 2015; 61:1312–1320. [PubMed: 24418637]
40. Lotfi S, Patel AS, Mattock K, Egginton S, Smith A, Modarai B. Towards a more relevant hind limb model of muscle ischaemia. *Atherosclerosis*. 2013; 227:1–8. [PubMed: 23177969]
41. Stacy MR, Yu da Y, Maxfield MW, Jaba IM, Jozwik BP, Zhuang ZW, et al. Multimodality imaging approach for serial assessment of regional changes in lower extremity arteriogenesis and tissue perfusion in a porcine model of peripheral arterial disease. *Circulation. Cardiovascular imaging*. 2014; 7:92–99. [PubMed: 24170237]
42. Pung YF, Chilian WM. Corruption of coronary collateral growth in metabolic syndrome: Role of oxidative stress. *World journal of cardiology*. 2010; 2:421–427. [PubMed: 21191543]
43. Engel WK, Hawley RJ. Focal lesions of muscle in peripheral vascular disease. *J Neurol*. 1977; 215:161–168. [PubMed: 69685]
44. Garcia M, Mulvagh SL, Bairey Merz CN, Buring JE, Manson JE. Cardiovascular disease in women: Clinical perspectives. *Circ Res*. 2016; 118:1273–1293. [PubMed: 27081110]
45. Pollak AW. PAD in women: The ischemic continuum. *Curr Atheroscler Rep*. 2015; 17:513. [PubMed: 25939674]
46. Duberstein KJ, Platt SR, Holmes SP, Dove CR, Howerth EW, Kent M, et al. Gait analysis in a pre- and post-ischemic stroke biomedical pig model. *Physiol Behav*. 2014; 125:8–16. [PubMed: 24286894]

CLINICAL RELEVANCE PARAGRAPH

Peripheral arterial disease (PAD) is a pandemic in need of novel pharmaceutical and regenerative medicine treatments. However, the clinical testing of novel therapies is best performed after dosing and delivery strategies have been identified in pre-clinical models. Unfortunately, there is not a suitable preclinical model of PAD. Here we characterize a novel porcine model of PAD that delivers ischemic myopathy to the affected limb through sustained depressions in perfusion. The objective of this study was to create and describe a novel, endovascular large animal model of PAD that may be useful in the testing of new pharmaceutical and cellular therapies for the of PAD.

Author Manuscript

Author Manuscript

Author Manuscript

Author Manuscript

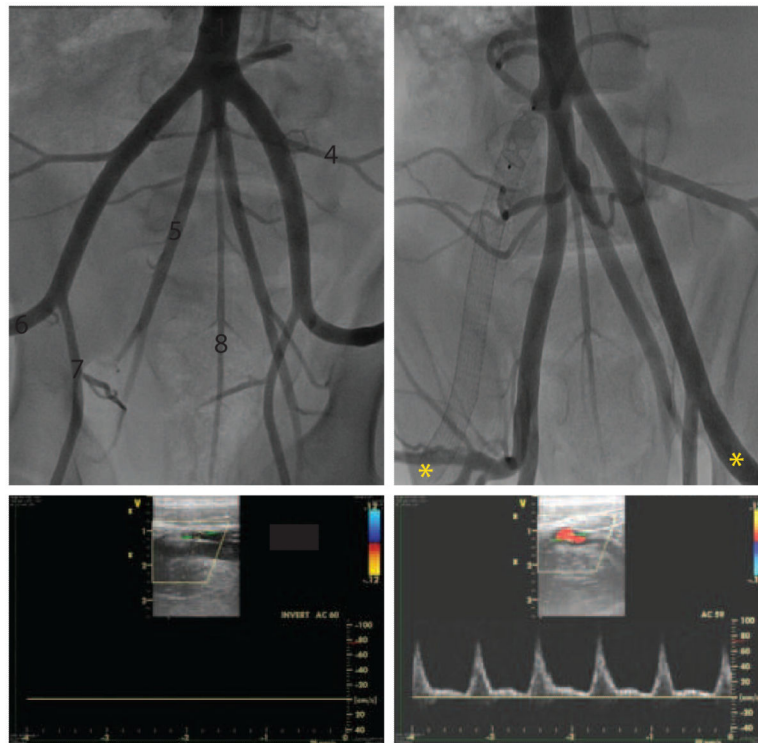


Fig 1. Angiographic images from endovascular occlusion procedure. **A**, Porcine pelvic arterial anatomy prior to occlusion – 1. aortic trifurcation, 2. external iliac artery (EIA), 3. common iliac artery, 4. lateral circumflex artery, 5. internal iliac artery (IIA), 6. common femoral artery, 7. profunda artery, 8. middle sacral artery. Note the IIAs originate from the common iliac artery (3), which is the middle branch of the aortic trifurcation. White dashed box denotes covered stent implantation site. **B**, Post-stent and vascular plug implantation. **C**, **D**, Doppler ultrasound data acquired in the distal EIAs (*) demonstrate flow cessation in right (ischemic) hind limb, while flow in left (non-ischemic) hind limb is maintained. Survival of the occluded limb is maintained through collateral flow into the popliteal artery via branches of the profunda artery (downstream of the IIA).

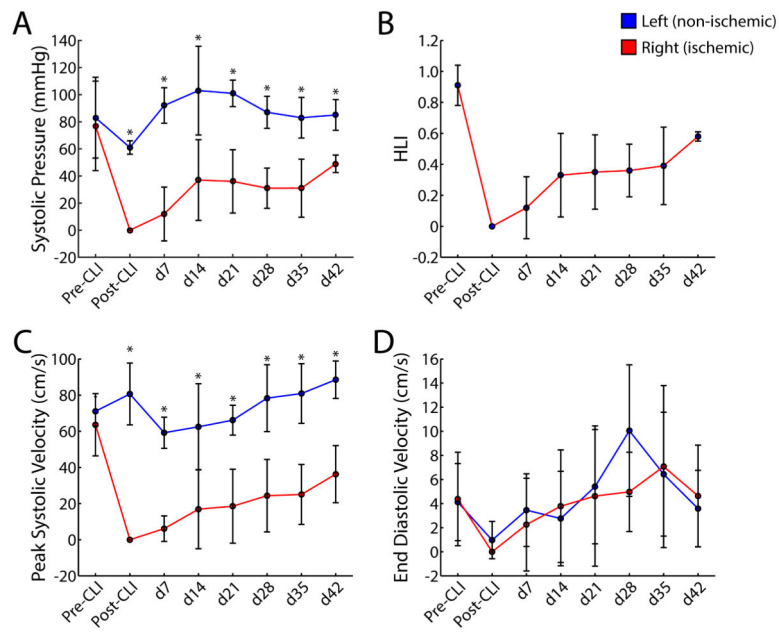


Fig 2. Hind limb hemodynamic parameters. **A**, Systolic blood pressure. **B**, Hind limb index (HLI; ratio of systolic pressures in occluded and normal limbs). Note that arterial pressures in occluded hind limb (right) remain depressed and stable over 7 weeks. **C**, Peak systolic velocity. **D**, End diastolic velocity. Data are means \pm SD. *P < 0.01. CLI: chronic limb ischemia.

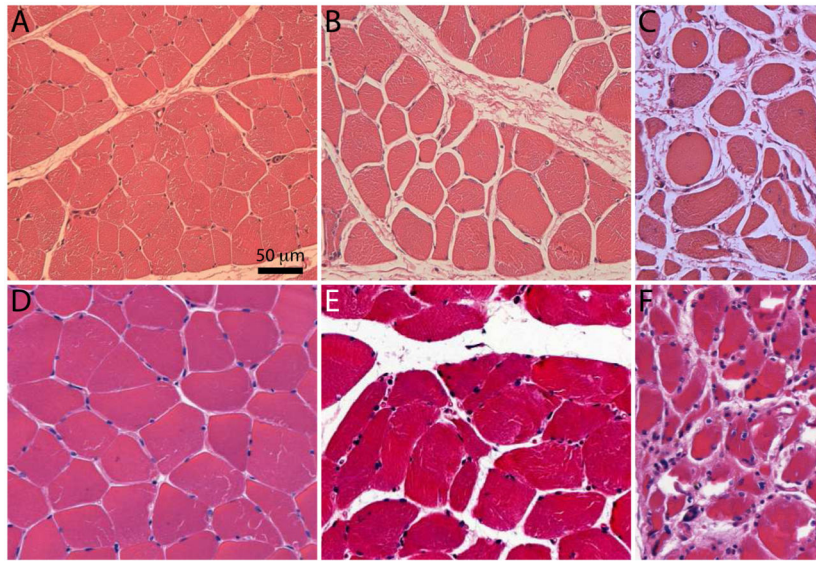


Fig 3. Representative micrographs of ischemic myopathy severity in Yorkshire swine and human gastrocnemius muscle. **A**, Normal histology of gastrocnemius tissue in control Yorkshire (myofibers exhibit regular polygonal shape, little size variation, and peripherally located nuclei). **B, C**, Varying degrees of ischemic myopathy in right hind limb (myofibers exhibit nonpolygonal round shape, large size variation, and centrally located nuclei; thickened endomysium). **D**, Normal histology of gastrocnemius tissue in control patient. **E, F**, Stage 2 and 4 clinical disease, respectively, in claudicant patients. Scale bar = 50 μ m.

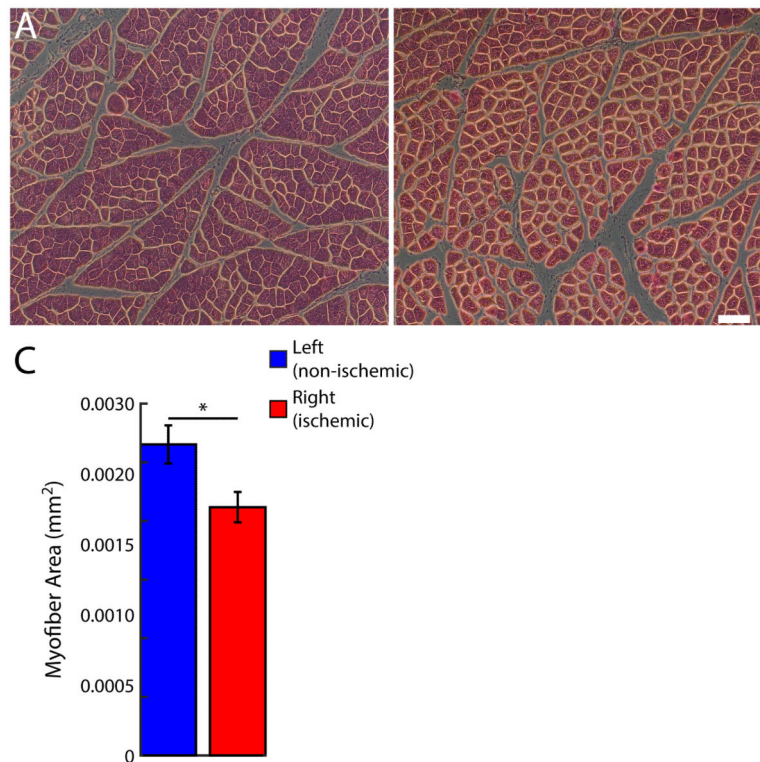


Fig 4. Hind limb ischemic myopathy in Yorkshire swine. **A, B**, Representative micrographs from left (non-ischemic) and right (ischemic) gastrocnemius muscle, respectively. Scale bar = 100 μ m. **C**, Myofiber area. Data are means \pm SD. *P < 0.05.

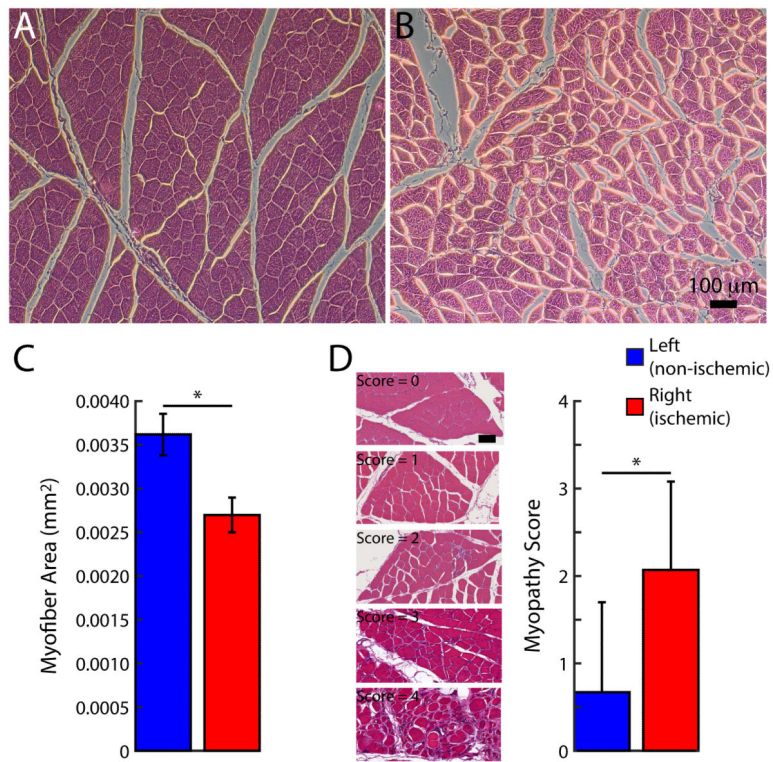


Fig 5. Hind limb ischemic myopathy in fat fed Ossabaw swine. **A, B,** Representative micrographs from left (non-ischemic) and right (ischemic) gastrocnemius muscle, respectively. Scale bar = 100 µm. **C,** Myofiber area. **D,** Histopathologic analysis of myopathy score and representative micrographs across scoring range. Scale bar = 50 µm. Data are means ± SD. *P < 0.05.

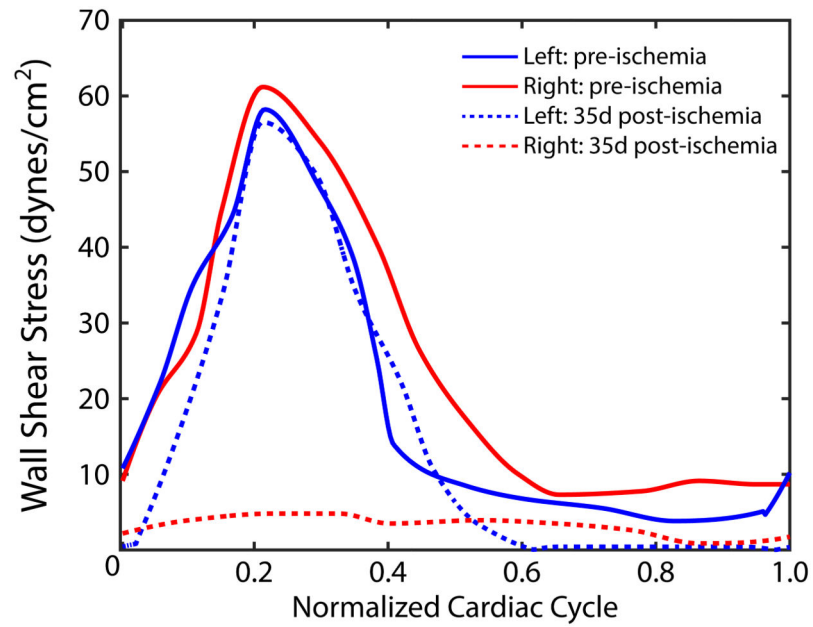


Fig 6. Wall shear stress (WSS) values in femoral arteries pre-ischemia and 35 days post-ischemia. At 35 days post-ischemia, WSS values in the left femoral artery (non-ischemic, dashed blue line) remained unchanged from pre-ischemic levels (solid blue line); however, WSS values in the right femoral artery (ischemic limb) at 35 days post-ischemia (dashed red line) exhibited very low values as compared to pre-ischemic levels (solid red line).

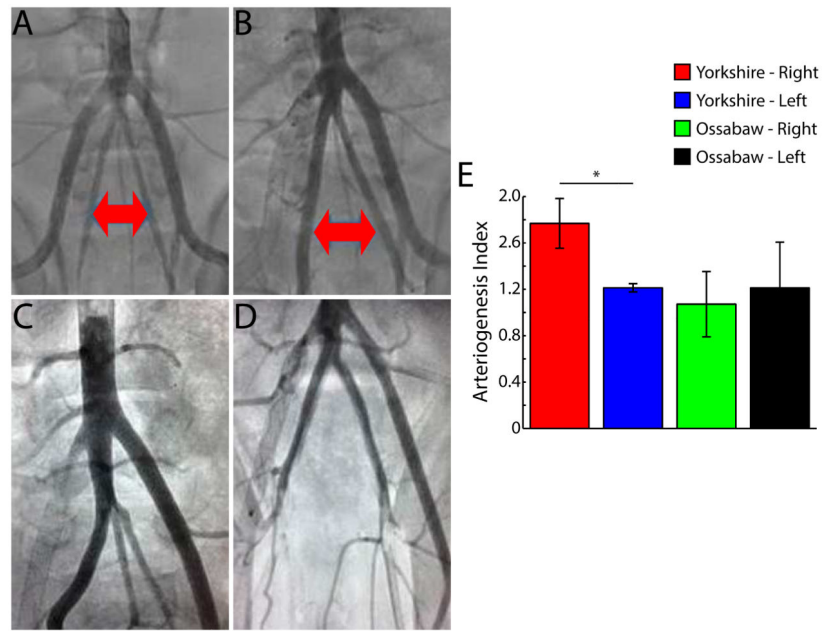


Fig 7. Arteriogenesis of ipsilateral internal iliac artery (IIA). **A, B**, Pre-occlusion and 5 week post-occlusion aortograms, respectively, in Yorkshire swine. Red arrows identify IIAs. **C**, Representative aortogram in Yorkshire swine at 5 weeks. Note difference in size of right (ischemic side) and left (non-ischemic side) IIAs **D**, Representative aortogram in Ossabaw swine at 5 weeks. **E**, Arteriogenesis index (ratio of diameters at pre-occlusion and 5 week post-occlusion) in Yorkshire and Ossabaw swine. Data are means \pm SD. * $P < 0.01$.